A Damping Control Method for a Matrix Converter with a Boost-up AC Chopper

Kazuhiro Koiwa
Major of Energy and Environmental Science
Nagaoka University of Technology
Nagaoka, Niigata, Japan
newkoiwa@stn.nagoakaut.ac.jp

Jun-ichi Itoh
Dept. of Electrical, Electronics and Information Engineering
Nagaoka University of Technology
Nagaoka, Niigata, Japan
itoh@vos.nagaokaut.ac.jp

***Abstract*— This paper proposes a circuit topology for a matrix converter with a boost-up AC chopper in the input stage. In order to suppress the input filter resonance, the authors have developed a stabilization control for the input current using a V-connection AC chopper. However, the input current is required as the signal for the damping control. In this paper, the damping control using the existing filter capacitor voltage is proposed. In order to verify effectiveness of the proposed damping control, the proposed circuit is demonstrated by a 1.8-kW prototype. As a result, it was confirmed that the input current THD can be suppressed approximately 72.5% improved by applying the input current-type or the filter capacitor voltage-type damping controls.**

Keywords- Matrix converter; V-connection AC chopper; damping control; Capacitor voltage

I. INTRODUCTION

A matrix converter (MC) which can convert an AC power supply voltage directly into an AC output voltage of variable amplitude and frequency without the large energy storages, such as electrolytic capacitors, have been actively studied recently [1-8]. The following advantages are found as compared with a back-to-back converter, which consist of a PWM rectifier and a PWM inverter; (i) light-weight and long-life time due to no large electrolytic capacitor in the main circuit (ii) high efficiency because of less switching devices in the turn-on current path. The MC is expected to apply in the future renewable energy field such as hybrid electric vehicle systems, the wind power generator systems and others.

However, one of the disadvantages of the MC is the voltage transfer ratio, which defines as the ratio between the output voltage and the input voltage, is being constrained to 0.866. Consequently, the output current of the MC is higher than that of the back-to-back (BTB) type converter, under the same output power. Even the motor can drive at rated frequency as the field-weakening control is applied. However, the output current is increased and the efficiency of the system is reduced. Further, the motor loss increases due to the higher motor current. Besides, the restricted voltage transfer ratio also limits the applications of the MCs. Therefore, in considering of applying the MC in the near future of power electronics field, the boost-up functionality is important.

In order to solve this problem, a Matrix-Reactance Frequency Converter (MRFC), which consists of a MC and an AC chopper, has been studied in [2-3]. Reference [2] and [3] shows that, the amplitude of the output voltage can control to an extension which is higher than that of the input voltage. However the MRFC requires many components including the boost-up reactor and capacitor. In addition, the control becomes complicated because the regular synchronizing between the MC and the chopper is required.

On the other hand, another MC which can boost-up the voltage is connected in the previous stage of the MC. In other words, conventional circuit is composed as back-to-back around the filter capacitor. If MC operated by direction of the boost-up voltage is selected, high efficiency is obtained. However, the number of this circuit is twice of MC. Thus, the costs become higher.

This paper proposes a circuit topology which connects a V-connection AC chopper [4] in the input stage of the MC that enables boost-up functionality. However, the input filter resonance occurs in the proposed circuit. In order to suppress the input filter resonance, the current-type damping control has been proposed in [5]. In this case, the current sensors are necessary for the damping control, which results the cost of the system becomes higher.

In this paper, the capacitor voltage-type damping control which uses the existing filter capacitor voltage as the input signal is proposed. The voltage sensors have already been used in the control of the MC and the commutations. Thus, the input filter resonance can be suppressed without the current sensors. The constitutions in this paper are following. At first, the damping gains are designed using the extent input current and capacitor voltage. Then, the two damping controls are compared in term of performances by the bode diagram. The proposed circuit is demonstrated by a 1.8-kW prototype. Additionally, the efficiency, input power factor and input current THD characteristics are measured. As these results, it is confirmed that the effectiveness of the proposed damping control is verified by experiment.

II. CIRCUIT TOPOLOGY

Fig.1-(a) shows the proposed circuit which connects a V-connection AC chopper in the input stage of the MC. The power device in the AC chopper uses eight IGBTs. The relationships between the input voltage v_{in} and the output voltage v_{out} is expressed by

$$v_{out} = \beta \cdot \lambda_{mc} \cdot v_{in} \quad (1),$$

where, λ_{mc} is the modulation index of the MC, β is the boost-up ratio of the chopper and v_{in} is the input voltage. Basically, the function of the AC chopper is simply boost-up the input voltage. Then it does not uses a feedback control for the filter capacitor since both the input side and the output side of the AC chopper are AC voltage. Therefore, the capacitor value does not dominate by the voltage control response and the current response for the input side in contrast with a BTB system. As a result, the V-connection AC chopper and its components do not dominate the size and the weight in comparison to the origin structure of a MC. In addition, the maximum output voltage of the proposed circuit is decided by the duty ratio of the AC chopper. It should be noted that the switches in the AC chopper do not operate when the voltage transfer ratio is lower than 0.866 of the input voltage. That is, at the range of low output voltage, the proposed circuit is able to obtain high efficiency similarly to the original MC.

Fig.1-(b) shows the block diagram of input filter without the input current stability methods. According to this block diagram, the transfer function between the input voltage and the capacitor voltage is expressed by (2).

$$G_{BMC} = \frac{v_c}{v_{in}} = \frac{\dfrac{1}{\beta \cdot LC}}{s^2 + \dfrac{1}{\beta^2 \cdot LC}} \quad (2)$$

Thus, it is confirmed that the input filter resonance occurs as the angular frequency is (3).

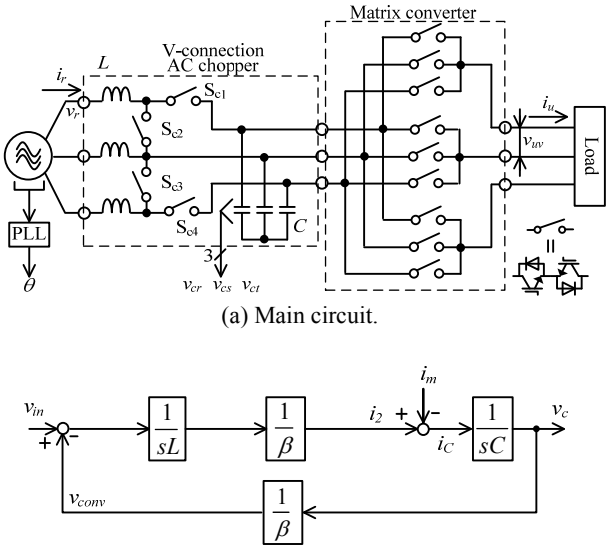

(a) Main circuit.

(b) Block diagram of input filter without input current stability methods.

Figure 1. Circuit configuration of proposed circuit.

$$\omega = \frac{1}{\beta\sqrt{LC}} \quad (3)$$

III. DAMPING CONTROL STRATEGY

A. Matrix Converter Control

Fig.2 shows the control block diagram of the proposed circuit. In this paper, the pulse pattern of the MC is generated by the virtual indirect control method [6-7]. The virtual indirect control method can separate into input current control and output voltage control. Thus, the conventional control method can be applied into each of the control. The input current command i_{cd}^* and i_{cq}^* are generated from the capacitor voltage in order to keep constant output power [8]. Thus, they are expressed by (4) and (5), respectively.

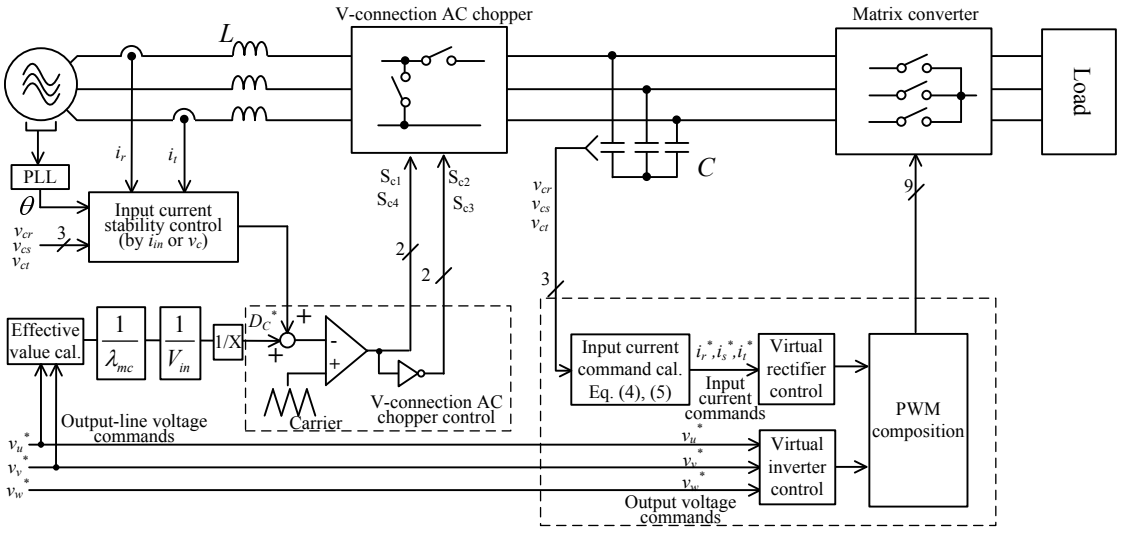

Figure 2 Control block diagram of proposed circuit.

$$i_{cd}^{*} = \frac{p \cdot v_{cd} - q \cdot v_{cq}}{v_{cd}^{2} + v_{cq}^{2}} \tag{4}$$

$$i_{cq}^{*} = \frac{p \cdot v_{cq} - q \cdot v_{cd}}{v_{cd}^{2} + v_{cq}^{2}} \tag{5}$$

where, p is the active instantaneous power command, q is the reactive instantaneous power command. Note that p is equal to 1, and q is equal to 0 in this paper.

Beside, in order to simulate constant power sources, automatic current regulation (ACR) has been introduced in the control of the MC.

B. Input Current Type Damping Control

The resonance between the input reactor and the filter capacitor occurs in the input stage. In general, in order to suppress the input filter resonance, the damping resistor is connected at the input filter. However, the efficiency is degraded because of the damping resistor loss. In contrast, the damping control can suppress the input filter resonance without degrading of the efficiency [9]. In case of the proposed circuit, we confirmed that the input filter resonance could not be suppressed by the damping control. There, the input current-type damping control is applied to the AC chopper.

Fig.3-(a) shows the control diagram of the damping control with the input current. The input currents are detected as signals to use damping control. Additionally, high pass filter (HPF) is used to decouple the oscillation component into the input current. The damping control is implemented on the d-q frame of the AC chopper control. The fundamental frequency component on the d-q frame becomes a constant value, i.e. DC signal. In addition, the harmonics components are appeared as ripple components. The distortion component of the input current is extracted by the HPF. After that, the distortion component is added to the chopper command D_c^{*}.

Fig.3-(b) shows the transfer function block diagram of the input current type damping control. K_v is the converter gain, which is defined as a maximum input voltage in the AC chopper. T_{HPF} is the time constant of HPF. Then, the transfer function from the input side of the AC chopper to the output side of the AC chopper is expressed by (6).

$$G_{damp\_I} = \frac{V_c}{V_{in}} = \frac{\frac{1}{\beta LC}s + \frac{1}{\beta LCT_{HPF}}}{s^3 + (\frac{1}{T_{HPF}} + \frac{K_v K_{d\_I}}{L})s^2 + \frac{1}{\beta^2 LC}s + \frac{1}{\beta^2 LCT_{HPF}}} \tag{6}$$

Assume that the damping control suppresses the oscillation component as same as connecting the damping resistor R. The transient response of the transfer function for the AC chopper with the damping resistor R is expressed by (7).

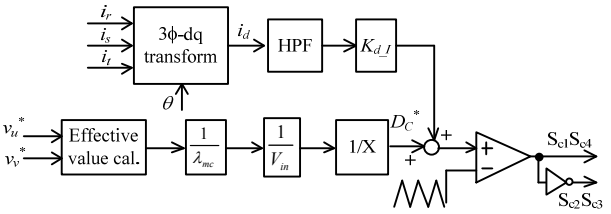

(a) Control diagram of AC chopper.

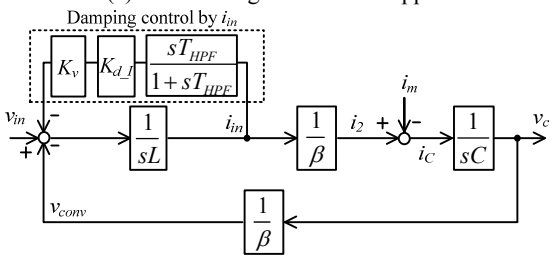

(b) Block diagram of input filter.

Figure 3. Input current-type damping control.

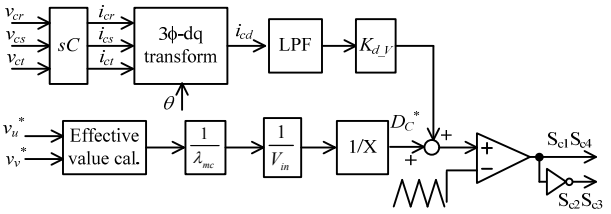

(a) Control diagram of AC chopper.

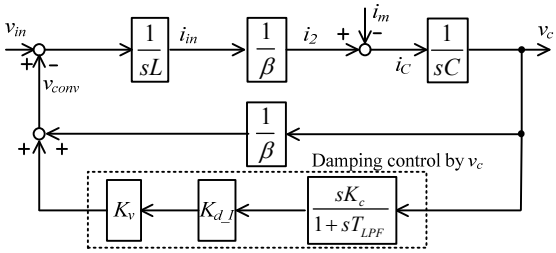

(b) Block diagram of the input filter.

Figure 4. Capacitor voltage-type damping control.

$$G_{resist} = \frac{V_{in}}{V_{out}} = \frac{\frac{R}{\beta \cdot L}s + \frac{1}{\beta \cdot LC}}{s^2 + \frac{R}{\beta^2 \cdot L}s + \frac{1}{\beta^2 \cdot LC}} \tag{7}$$

When the transfer function of the equation (6) is equaled to (7) at resonance frequency, the damping gain K_{d_I} is expressed by (8).

$$K_{d\_I} = \frac{2L\sqrt{\beta^2 + \frac{T_{HPF}^{2}}{LC}}}{\beta K_v T_{HPF}} \cdot \frac{\zeta}{\sqrt{4\zeta^2 + \beta^2}} \tag{8},$$

where, ζ is the damping factor which expresses by (9).

$$\zeta = \frac{R}{2\beta}\sqrt{\frac{C}{L}} \tag{9}$$

Note that the input reactor of the proposed circuit is virtually changed due to the AC chopper [10].

C. Capacitor Voltage Type Damping Control

In the input current-type damping control, the effect of suppression of resonance distortion can be confirmed. However, in this damping control method, the current sensors are necessary to apply in the damping control. As a result, the cost of the proposed system is higher due to increasing amounts of the current sensor. In one hand, the damping control method using the existing filter capacitor voltage is proposed.

Fig.4-(a) shows the control diagram of the filter capacitor voltage. The operation of the proposed block damping control is as following. At first, the capacitor current i_c is estimated by differentiation from the capacitor voltage v_c. After that, d-axis current is obtained on d-q frame. In addition, switching ripple included in d-axis current is extracted by using a low-pass filter (LPF). It is multiplied to the damping gain K_d. Finally, the distortion component is added to the chopper command D_c^*. However, the differentiation cannot use due to the noise. In this paper, instead of the differentiation, a HPF is used as pseudo differentiation. The proposed damping control is operating for the distortion component as the feedback regulator. On the other hand, the fundamental component is not affected. For this reason, the chopper control does not require the high speed response. It means that the filter capacitor and the boost-up reactor are not dominated by the control response of the input current and the capacitor voltage. Then, the transfer function from the input side of the AC chopper to the output side of the AC chopper is expressed by (10).

$$G_{damp\_V} = \frac{\frac{1}{\beta LCT_{LPF}}s + \frac{1}{\beta LC}}{s^3 + \frac{1}{T_{LPF}}s^2 + (\frac{K_v K_{d\_V}}{\beta L} + \frac{T_{LPF}}{\beta^2 LC})s + \frac{1}{\beta^2 LC}} \tag{10}$$

Similar to the design by the input current-type damping control, when the transfer function of the equation (10) is equaled to (7) at resonance frequency, the damping gain K_{d_V} is expressed by (11).

$$K_{d\_V} = \frac{2\zeta}{\beta K_v K_c}\cdot\sqrt{\frac{\beta^2 LC + {T_{LPF}}^2}{4\zeta^2 + 1}} \tag{11}$$

Accordingly, the damping gain can be designed from required damping factor by (11).

Fig.5 shows the gain characteristics comparison between without the damping control and with two damping control. Note that each frequency response is calculated by (2), (6) and (10). In addition, Table 1 shows the calculation parameters. As a result, the proposed circuit without the damping control is unstable due to input filter resonance. In addition, the voltage

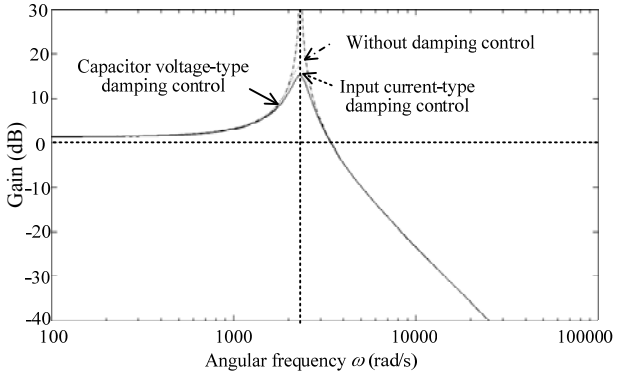

Figure 5. Gain characteristics.

Table 1. Calculation parameters.

Input phase voltage	115 V	Input current-type damping control	
Output line voltage	200 V	Damping gain K_{d_I}	0.014
Output power P_o	1.8 kW	Time constant of HPF T_{HPF}	3.18ms
Boost-up ratio of AC chopper β	1.15	Capacitor voltage-type damping control	
Input reactor	10.5 mH	Damping gain K_{d_V}	0.02
Filter capacitor	13.2 μF	Time constant of HPF T_{HPF}	13.2 μs
Resonance angular frequency ω_c	2340 rad/s	Converter gain K_v	282 V

gain without the damping control is approximately 145dB. On the other hand, the maximum voltage gain with the input current-type damping control or the capacitor voltage-type damping control is 17.5dB and 15dB. Thus, it can be confirmed that the voltage gain between the input side and output side of the AC chopper is approximately improved by 130dB. Moreover, the input filter resonance can be suppressed without degrading the voltage response. In additionally, it can be confirmed that the suppression effects of the input filter resonance of the capacitor voltage-type damping control is obtained as same as the input current-type damping control. Thus, the resonance distortion on the input current can be suppressed without the current sensors.

IV. Simulation Results

Fig.6 shows the operation waveform of the proposed circuit with the input current type damping control. Table 2 shows the simulation conditions. In the simulation, in order to simulate constant power sources, the current resources are used in the output load. Note that the damping control is applied after 0.1ms on simulation. Accordingly, the distortion of the resonance frequency components occurs in the input current waveform while the damping control is not applied. The input current total harmonic distortion (THD) is 38.2%.

Fig.7 shows the operation waveforms with the filter capacitor voltage-type damping control. Table 2 shows the simulation conditions. As a result, the resonance distortion in the input current is suppressed in steady state. Moreover, it is confirmed that the output power P_o is constant. The input current THD is 3.3%. Thus, the input current THD can be 35% decreased with the damping control.

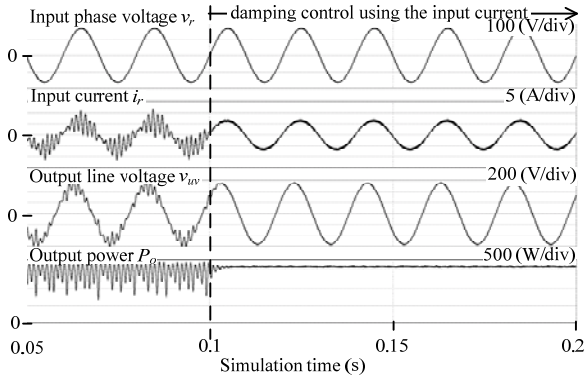

Figure 6. Simulation result of the input current type damping control.

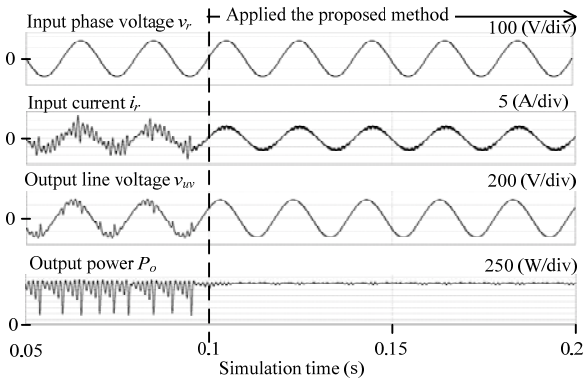

Figure 7. Simulation result of the capacitor voltage type damping control.

V. EXPERIMENTAL RESULTS

Fig.8 shows the photo of experimental platform. As IGBT, 1MBH50D-060 (Fuji electric corp.) and SK-80-GM-063 (SEMIKRON Inc.) are used in the prototype. In order to protect the switching devices from the surge voltage, dynamic clamp circuit (No.1 in this photo) and snubber circuit (No.2 is this photo) are used as the protect circuit.

Fig.9 shows the experimental result without the damping control. Table 2 shows the experimental conditions. In the proposed circuit, the input filter resonance does not occur because of the chopper loss becomes a role of the damping resistor. There, it considered that a generator was connected in the input stage of the proposed circuit. Thus, the input reactor is connected 10.5mH (16.5%). Moreover, the PI-control gains in ACR were calculated from the standard transfer function. Additionally, the output line voltage v_{uv} was observed by using LPF which the cut-off frequency is equal to 1.5 kHz. Besides, since the MC uses bi-directional switches, are required to apply with commutation pattern to prevent the source and load from open circuit and short circuit. In this paper, the 4-step commutation method is applied in the proposed circuit [11]. And also, the voltage information of the filter capacitors is used in this commutation. According to this result, the input current THD and the output line voltage are 23.5% and 7.48%, respectively. Thus, the waveforms are distorted by the input filter resonance.

Fig.10 shows the experimental results with the input current type damping control. Accordingly, the resonance distortion in the input current is suppressed by applying the damping control. It is accomplished that the input current THD and the output line voltage THD are 10.3% and 3.52%, respectively. From these results, it is confirmed that the input current THD and the output line voltage THD can be improved 56.2% and 47% in contrast with the damping control is not applied. Incidentally, the damping factor ζ is obtained by (12) from (8).

$$\zeta = \frac{1}{2}\frac{\beta K_v K_{d\_I} T_{HPF}}{\sqrt{\beta^2 L^2 + \frac{L \cdot T_{HPF}^{\ 2}}{C} - \beta^2 K_v^{\ 2} K_{d\_I}^{\ 2} T_{HPF}^{\ 2}}} \tag{12}$$

According to equation (10), the damping factor by the input current-type damping control is 0.73 calculated in this

Table 2. Simulation and experimental conditions.

		Simulation	Experiment
Input phase voltage V_{in}		115 V	
Input frequency f_{in}		50 Hz	
Carrier frequency f_s	Chopper	10 kHz	
	MC		
Input reactor L		2 mH	10.5 mH
Filter capacitor C		13.2 μF	13.2 μF
Boost-up ratio of the chopper β_c		1.155	
Damping gain K_{d_V}		0.5	4.0
Load		Constant current source	R-L load (12.5Ω, 5mH)

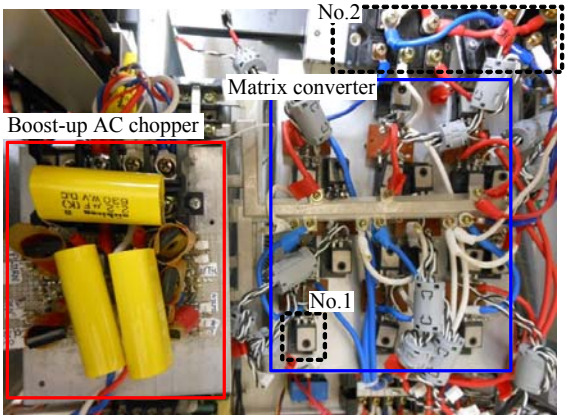

Figure 8. Experimental platforms.

experimental result. Note that calculated the damping factor is only by the damping control. However, the distortion can be suppressed by the damping control as well as the chopper loss. Therefore, the input current waveform is distorted because of the input filter resonance is excessively compensated by the damping control in the experiment.

Fig.11 shows the experimental results with the filter capacitor voltage-type damping control. The resonance distortion can be suppressed as well as the input current type damping control. The input current THD and the output line voltage THD are 6.47% and 5.36%, respectively. From these results, it is confirmed that the input current THD and the output line voltage THD can be improved by 72.5% and 28.3% in contrast with the case damping control is not applied. Similar to the input current type damping control, the damping factor is expressed from (11) by (13).

$$\zeta = \frac{1}{2}\frac{\beta K_v K_{d\_V} K_c}{\sqrt{\beta^2 LC + {T_{LPF}}^2 - \beta^2 {K_v}^2 {K_{d\_V}}^2 {K_c}^2}} \quad (13)$$

According to equation (13), the damping factor by the filter capacitor voltage-type damping control is 0.012 calculated in this experimental result. The damping factor is lesser in contrast with the input current-type damping control. Therefore, the input current waveform is sinusoidal because the input filter resonance is not excessively compensated.

Fig.12 shows harmonic components of the input current without the damping control and with two damping controls. At first, in comparison between the results with/without the damping control, almost of the harmonic components in the both results with the damping control is reduced than the results without the damping control. Therefore, the effectiveness of damping control is confirmed to control the stabilization of the input current. Next, the filter capacitor voltage-type damping control is compared with the input current-type. As a result, it is confirmed that the suppression effect of the resonance distortion is similar to the input current type damping control. However, the even order components of the input current type damping control is larger than that of the proposed damping control. This is because the input filter resonance is excessively compensated by the input current type damping control and the chopper loss.

Fig.13 shows the efficiency characteristics. Note that the output line voltage is 170V constantly. In addition, in order to change the output power, the load resistance is changed. According to this result, the efficiency is improved by applying the damping control. This is because the harmonic loss is degraded due to suppression of the resonance distortion. Then, the maximum efficiency of the proposed circuit is 93.83% at 1.0-kW load.

Fig.14 shows the input power factor characteristics. According to the result, the input power factor by applying each damping control is higher. This is because the leading current becomes larger due to harmonic component in the input current. Then, it can be achieved that the maximum input power factor is 0.988 as the output power is 1.0 kW.

Fig.15 shows the input current THD characteristics. Note that the gains of ACR were designed from the standard transfer function. In this experiment, the damping gain of the input current-type damping control K_{d_I} is 0.5. As a result, it can be achieved that the input current by the input current-type damping control is sinusoidal in comparison with Fig.10. According to the result, the input current THD is approximately 30% and 55% improved by applying each damping control. However, effect of the resonance suppression is decreased, with increasing the output power. This is because the AC chopper loss which rolls in effect of the damping is increased with increasing the output power. Furthermore, the input current THD with the input current-type damping control is lower than that of the capacitor voltage-type damping control. Thus, it is confirmed that the effect of the resonance suppression by the input current-type damping control is higher in comparison with the capacitor voltage-type damping control. However, the harmonic distortion can be suppressed by the capacitor voltage-type damping control without the current sensor. Therefore, it is not necessary to add extra current

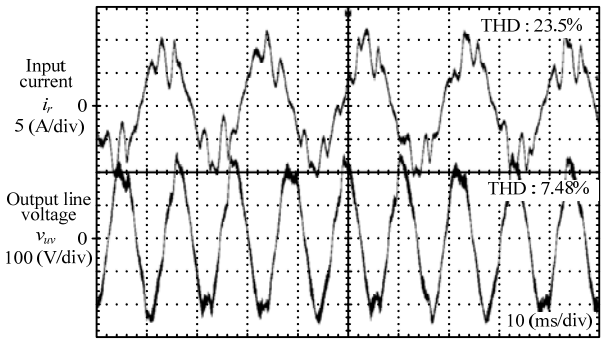

Figure 9. Experimental result without damping control.

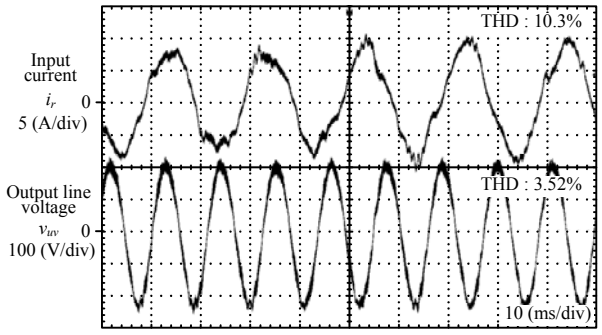

Figure 10. Experimental result with input current-type damping control.

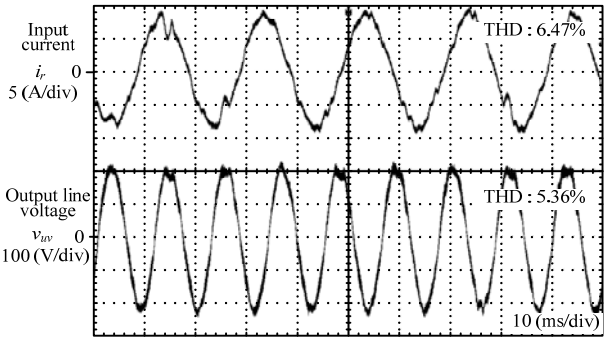

Figure 11. Experimental result with capacitor voltage-type damping control.

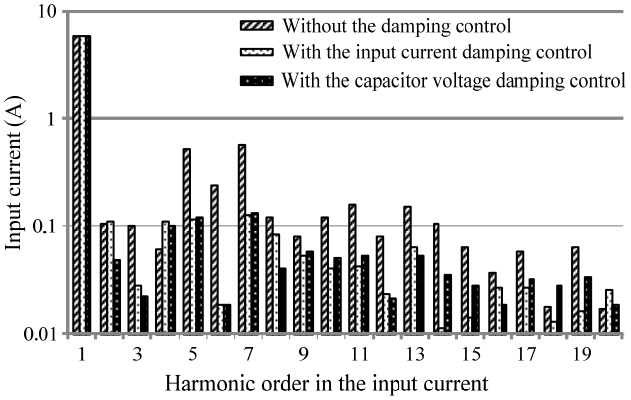

Figure 12. Harmonic components of input current.

sensors and detection circuit in the proposed circuit, which as a result can reduce the cost of the system.

VI. CONCLUSION

In this paper, the input current stability control was proposed without the detection of the input current and the output line voltage. The damping control can suppress the input filter resonance without degrading the efficiency. There, the damping control was applied in the AC chopper by the capacitor voltage.

The effect of resonance suppression of two damping controls was compared without the damping control by the bode diagram. As a result, it could be confirmed that the effect of resonance suppression of the proposed damping control was obtained as same as the conventional damping control.

The proposed circuit with the damping control was demonstrated by a 1.8-kW prototype. As a result, it confirmed that the input current THD and the output line voltage THD could be reduced by 72.5% and 28.3%, respectively. Then, the damping factor is 0.012. Moreover, it could be revealed that the efficiency and the input power factor were improved by the damping control. Then, it could be accomplished that the maximum efficiency and the input power factor are 93.83% and 0.988, respectively. Additionally, it could be confirmed that the effect of the resonance suppression by the input current-type damping control is higher in comparison with the proposed damping control. However, the harmonic distortion can be suppressed by the capacitor voltage-type damping control without the current sensor. From these results, the resonance distortion could be suppressed by the proposed damping control without additional current sensors.

In future works, the damping gain will be optimized. Besides, effectiveness of the damping controls will be verified in the motor load.

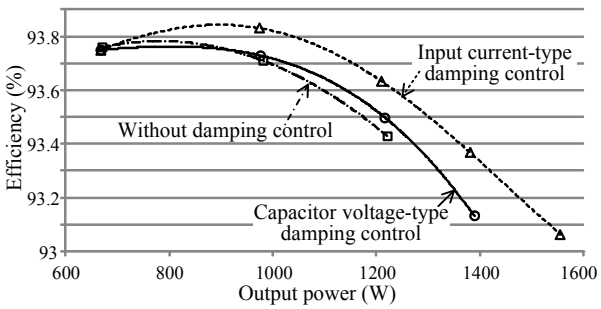

Figure 13. Efficiency characteristics.

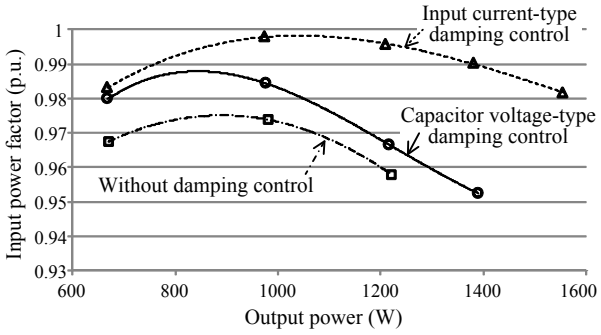

Figure 14. Power factor characteristics.

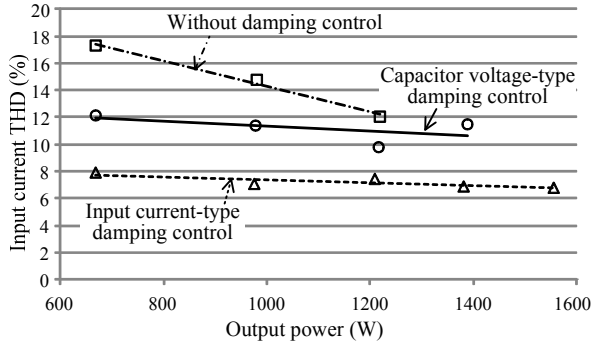

Figure 15. Input current THD characteristics.

REFERENCES

[1] P. W. Wheeler, J. Rodriguez, J. C. Clare, L. Empringham: "Matrix Converters: A Technology Review" IEEE Transactions on Industry Electronics Vol. 49, No. 2, pp274-288, 2002.

[2] Zbigniew Fedyczak, Pawel Szczesniak, Igor Korotyeyev; "New Family of Matrix-Reactance Frequency Converters Based on Unipolar PWM AC Matrix-Reactance Choppers"EPE-PEMC 2008, P170 pp.236-24

[3] Z. Fedyczak, P. Szczesniak, M. Klytta: "Matrix-Reactance Frequency Converter Based on Buck-Boost Topology", EPE-PEMC 2006, Vol. , No. , pp. 763-768 (2006)

[4] J. Itoh, H. Tajima, H. Ohsawa: "Induction Motor Drive System using V-connection AC Chopper", IEEJ Trans., Vol. 123, No. 3, pp. 271-277 (2003)

[5] K. Koiwa, J. Itoh, "Experimental Verification for a Matrix Converter with a V-connection AC Chopper," EPE2011, pp. 1-10 (2011)

[6] J. Itoh, H. Kodachi, A. Odaka, I. Sato, H. Ohguchi, H. Umida: "A High Performance Control Method for the Matrix Converter Based on PWM generation of Virtual AC/DC/AC Conversion", JIASC IEEJ, Vol. , No. , pp. I-303-I-308 (2004)

[7] J. Itoh, I. Sato, H. Ohguchi, K. Sato, A. Odaka and N. Eguchi: "A Control Method for the Matrix Converter Based on Virtual AC/DC/AC Conversion Using Carrier Comparison Method", IEEJ Trans., Vol.124-D, No.5, pp.457-463 (2004)

[8] I. Sato, J. Itoh, H. Ohguchi, A. Odaka, and H. Mine: "An Improvement Method of Matrix Converter Drives Under Input Voltage Disturbances", IPEC-Niigata, pp. 546–551 (2005)

[9] Junnosuke Haruna and Jun-ichi Itoh, "A Control Strategy for a Matrix Converter under a Large Impedance Power Supply," Power Electronics Specialists Conference 2007, pp. 659-664.

[10] T.Shinyama, M. Kawai, A. Torii, A. Ueda: "Characteristic of an AC Chopper Circuit with LC Filters in the Input and Output Side", IEEJ Trans., Vol. 125, No. 3, pp. 205-211 (2005)

[11] K. Kato, J. Itoh: "Development of a Novel Commutation Method which Drastically Suppresses Commutation Failure of a Matrix Converter," Trans.IEEJ,Vol.127-D,No.8,pp.829-836,2007